

**ICSV14**  
Cairns • Australia  
9-12 July, 2007



## **DETERMINATION OF ACOUSTIC PROPERTIES FOR OPEN DUCT TERMINATION IN HOT JET CONDITIONS USING FEM SIMULATION**

Hans Rämmal<sup>1</sup> and Jüri Lavrentjev<sup>1</sup>

<sup>1</sup> Department of Automotive Engineering, Tallinn University of Technology  
Ehitajate tee 5, Tallinn, 19086, Estonia  
[hansra@kth.se](mailto:hansra@kth.se)

### **Abstract**

Determination of the acoustical properties for hot flow duct openings is a classical problem in acoustics. The importance of this issue usually becomes apparent when for instance noise radiation from engine exhaust systems or burner chimneys is considered. In the present study a finite element method (FEM) simulation has been carried out to investigate the effects of high temperature media on the sound propagation through open duct termination. This paper is an extension for the recent experimental work performed by paper authors on acoustical properties of duct terminations exhausting hot gas. In order to simulate the experimental conditions, commercial FEM software COMSOL has been used. The acoustic pressure reflection coefficient of the duct termination is calculated from the complex pressures simulated at the location of two microphones in the test-duct model. Two geometrically different model configurations, based on experimental observations, are studied. The numerical results obtained from simulations are compared to the experimental ones and good agreement between the data is observed.

### **1. INTRODUCTION**

The acoustical behavior of a circular duct termination exhausting hot flow has recently been investigated by authors of the paper both experimentally [1] and by implementing Munt's theoretical model [2].

The objective of the present study was to compose a FEM model that simulates these experimental conditions. The model was developed to test the ability to implement simple FEM model for determination of passive acoustic properties of flow duct elements in low Mach number and low Helmholtz number conditions. Furthermore to verify the experimentally obtained results, it was intended for successive development to perform analysis on various duct termination geometries and flow conditions.

The experiments for the acoustical pressure reflection described in [1] were carried out by using a thin walled steel duct with circular cross-section area. The duct was mounted vertically in a room and hot air flow through the test section was generated by electrical

blowers and surface heating elements. The reflection coefficient was determined using the two microphone approach. A simplified layout of the experimental set-up used for the experiments is presented in Fig. 1. In order to investigate the temperature distribution of the flow and the shape of the exhausting jet, flow visualization experiments together with temperature mapping around the opening were carried out (see Section 2). This information was primarily important for composition the FEM models.

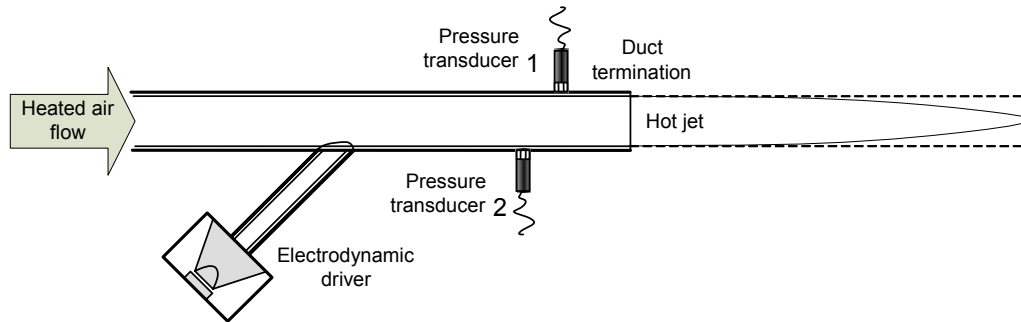


Figure 1. A simplified layout of the setup used for experiments in [1] and followed by the FEM model

Following the experimental conditions and corresponding test duct geometry a three dimensional FEM model was created using finite element method software COMSOL. In order to analyze an influence of variations in the jet geometry two different models – one with cylindrical and another with conical jet were tested. An overview of the modelling procedure is provided in Section 3.2.

Two microphone technique (see Section 3.1) was followed to determine the acoustical pressure reflection coefficient by using the complex pressures directly obtained from FEM simulations. The FEM simulation procedure with the model described in Section 3.2 was repeated at discrete frequencies selected to cover the range from 10 to 3000Hz. Three jet temperatures (100, 300 and 500°C) were selected for the simulation. Since the flow velocity was low during the experiments ( $M < 0.01$ ) the flow effects were neglected in this model. The latter simplification provides substantially easier modelling process together with less demanding computational effort.

In Section 4 the numerical results obtained for the analyzed temperature conditions are presented. The experimental results for the same jet temperatures are included for comparison.

## 2. TEMPERATURE MAPPING AND FLOW VISUALIZATION

The flow visualization was performed by implementing an infra-red (IR) imaging camera (Flir systems, Thermacam S65). In order to capture hot jet using the IR camera with reasonable clarity, smoke particles were generated in the flow by spraying oil into the hot test section. Despite of roughly cylindrical shape of the jet observed (see Fig. 2) a tendency to conicity can still be found at a distance about 0.25m from the opening. It can be noted here that the considerable density difference between the jet and the surrounding media (about 2 times for 300°C jet exhausting into room temperature air) normally leads to the phenomena known as accelerated flow. In such a flow condition even a decrease in jet diameter can be expected soon after passing the duct lips. The latter seems to be in agreement with the images

photographed and can be noticed on Fig. 2, up to around 0.2m from the duct opening.

Additionally to IR-imaging the temperature measurements using a dual K-type tripod mounted thermometer (TES 1312) were carried out in the region around the duct exit. The temperature readings were obtained by following a grid (see Fig. 2) that extended up to 1m from the termination along the duct central axis and up to 0.4m in radial direction. Assuming symmetry, the readings were taken only on one side of the plane. An example of the results obtained from this test is shown in Fig. 3. As can be seen the influence of the hot jet on surrounding room temperature (25°C) did not extend further than around 0.2m (about 4 duct diameters) in axial direction from the duct central axis.

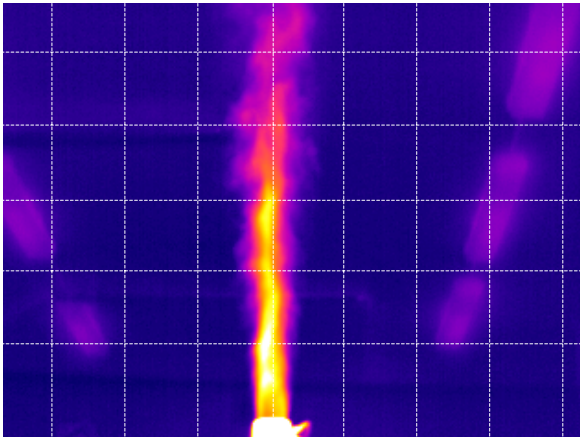


Figure 2. An example of IR camera image captured during flow visualization experiments; Average exit temperature:  $t=300^{\circ}\text{C}$ , flow velocity:  $v=2.5\text{m/s}$ ; the  $0.1 * 0.1\text{m}$  grid represents the spacing for the temperature readings depicted on Fig. 3.

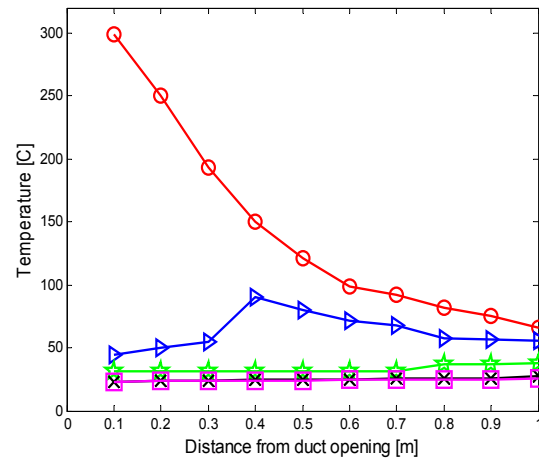


Figure 3. Temperature distribution near the test duct termination;  $t = 300^{\circ}\text{C}$ ,  $v=2.5\text{m/s}$ ; distances from central axis: 0 m (red circles), 0.1 m (blue triangles), 0.2 m (green stars), 0.3 m (black X-s), 0.4 m (magenta squares).

### 3. SIMULATION PROCEDURE

#### 3.1 Determination of the acoustic pressure reflection coefficient

Assuming linear and passive termination in the positive  $x$ -direction (see Fig. 4) and concerning only a plane wave state, the reflection coefficient can be defined in that direction as:

$$R_1(f) = \frac{p_{1-}(f)}{p_{1+}(f)}, \quad (1)$$

where  $p_{1-}, p_{1+}$  is the acoustic field generated by the simulation model at microphone 1 cross-section. Following the two microphone method, the incident and reflected pressure wave

amplitudes  $p_{1+}(f)$  and  $p_{1-}(f)$  can be calculated at the reference cross-section using two microphone positions (see Fig. 1) as follows:

$$p_1(f) = p_{1+}(f) + p_{1-}(f), \quad (2)$$

$$p_2(f) = p_{1+}(f) \exp(-ik_+s) + p_{1-}(f) \exp(ik_-s), \quad (3)$$

where  $p$  is the acoustic pressure,  $f$  is the frequency,  $k = 2\pi f / c$  is the wave number,  $c$  is the speed of sound,  $s$  represents the microphone separation, - and + denote the pressure waves propagating in neg. and pos. direction relative to the  $x$ -axis,  $k_- = k / (1 - M)$ ,  $k_+ = k / (1 + M)$  and  $M$  is the Mach number. Indexes 1 and 2 denote the microphone positions. Furthermore, in the current paper the complex acoustic pressures  $p_1(f)$  and  $p_2(f)$  are the input parameters obtained from FEM simulation for the reflection coefficient calculation described here.

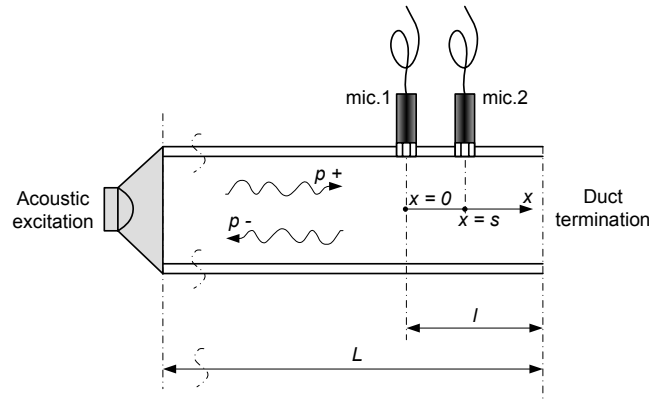


Figure 4. Model configuration according to the two microphone technique.

By combining the equations (2) and (3), the expressions for  $p_{1+}(f)$  and  $p_{1-}(f)$  will be obtained as follows:

$$p_{1-}(f) = \frac{p_2(f) - p_1(f) \exp(-ik_+s)}{\exp(ik_-s) - \exp(-ik_+s)} \quad (4)$$

$$p_{1+}(f) = \frac{p_1(f) \exp(ik_-s) - p_2(f)}{\exp(ik_-s) - \exp(-ik_+s)} \quad (5)$$

In order to determine the reflection coefficient at the duct termination cross-section, it is necessary to move  $R_1$  to this location. This can be done by using the equation

$$R = R_1 \exp(i \cdot (k_+ + k_-) \cdot l). \quad (6)$$

### 3.2 The simulation model

A commercial finite element method software (COMSOL Multiphysics 3.3) was used in order to obtain the complex acoustic pressures  $p_1(f)$  and  $p_2(f)$  at pressure transducer cross-sections by simulations. Two geometrically different jet models were tested. First a cylindrical model for the hot jet was composed as shown in Fig. 5. Second model tested was with conical jet geometry (see Fig. 6). The conicity of the jet was chosen as large as  $16^\circ$  in order to investigate the effect of conicity on the results.

For both 3-D models created, the dimensions of the test-duct model followed the ones of the experimental pipe. The duct walls (with 2mm thickness) were defined as acoustically hard, which means that the gradient of the sound pressure field in the normal direction of the duct is always zero. In order to keep the calculation time reasonable, the space surrounding the duct termination model (see Fig. 5) was reduced to a prism (height  $h=1.3\text{m}$ , and the base area  $A=1\text{m}^2$ ).

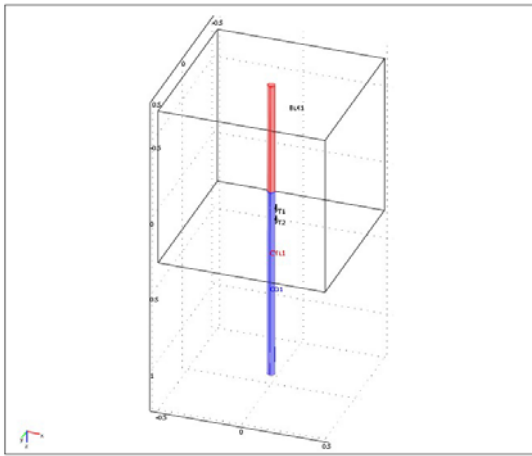


Figure 5. An image of the FEM model with cylindrical jet geometry. The duct termination is modelled inside the surrounding volume.

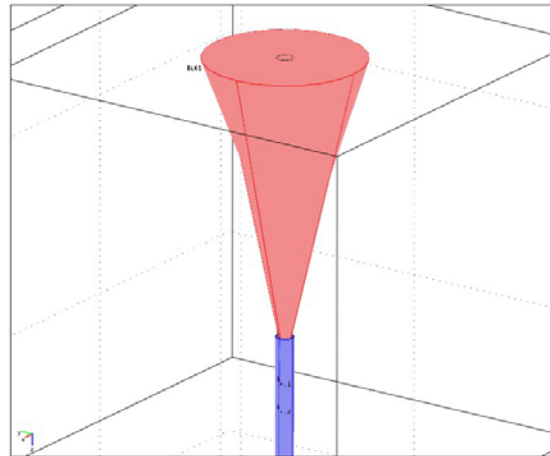


Figure 6. An image of the FEM model with conical jet geometry.

Properties of air at room temperature ( $25^\circ\text{C}$ ) and normal pressure were defined for the surrounding volume. A radiation condition was determined to represent the boundary conditions of the prism surface areas. This boundary condition models a surface where all incident waves are transmitted outside of the prism and not being reflected back to the duct, as could be expected in the experimental case.

The duct termination was located at the height of 0.3m from the bottom surface along the vertical central axis of prism.

Uniform acoustical conditions inside the jet were defined for every simulated temperature case. The hot jet was modelled to fill the test duct internal volume completely and to extend out of the termination up to the limiting surface of the surrounding prism (1m from the termination) either continuing the cylindrical shape or conically (see Figs. 5 and 6). A continuity condition was defined to represent the boundary conditions at the surface between the jet and the surrounding media.

At the bottom surface of the duct the fluctuating sound pressure providing the acoustic

excitation was defined to have a value of 20Pa. But since this is a linear model this value can be scaled to any other appropriate value without affecting the results. The simulations were run for eleven excitation frequencies to cover the range from 10Hz to 3kHz. After the solution is computed it is necessary to post-process the results in order to obtain the acoustic pressures  $p_1(f)$  and  $p_2(f)$ . These values are found by evaluating the complex pressures at the coordinates of two pre-determined points on the duct inner surface. These two points represent the positions of the pressure transducers in the duct during the corresponding experiments.

The following task was to insert these simulated pressure values into the calculation module, described in Section 3.1, to determine the pressure reflection coefficient. This procedure was repeated for each of the excitation frequency.

### 4. RESULTS

The numerically determined magnitude and phase of the reflection coefficients for all the modelled jet temperatures are presented in Figs. 7-12. The corresponding results obtained experimentally are included in comparison. The agreement between the results is good for all the temperatures. The figures show that the two geometrically different jet models produce relatively similar results. However, it can be noticed that in some cases the results from the cylindrical model are in marginally better correlation with the measured ones.

In Fig. 13 the reflection coefficient magnitude is presented for 100°C and 500°C jet temperatures. In this figure the results obtained by Munt's theoretical model are brought into comparison. These analytical results confirm the numerical and experimental ones.

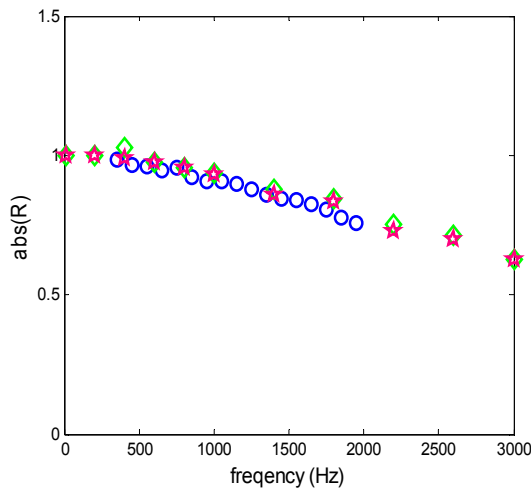


Figure 7. The magnitude of the reflection coefficient for duct open termination;  $t = 100\text{ }^\circ\text{C}$ , Experiments (blue circles), FEM - conical model (green diamonds), FEM - cylindrical model (pink stars)

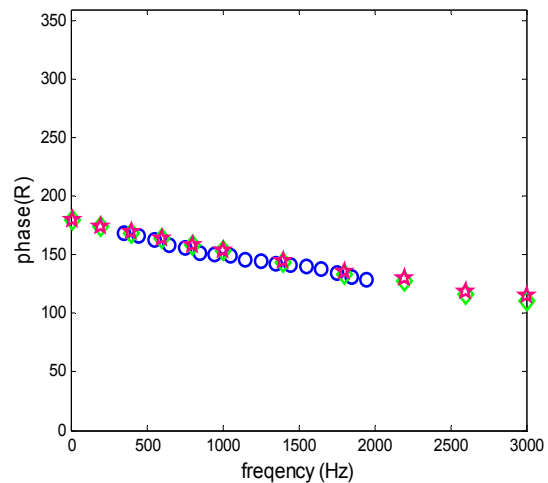


Figure 8. The phase of the reflection coefficient for duct open termination;  $t = 100\text{ }^\circ\text{C}$ ; experiments (blue circles), FEM - conical model (green diamonds), FEM - cylindrical model (pink stars)

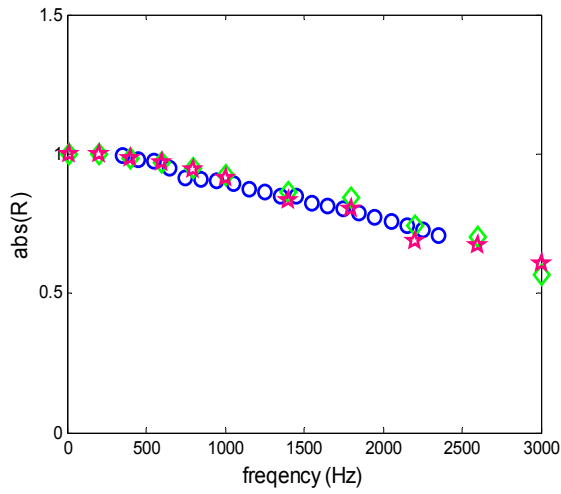


Figure 9. The magnitude of the reflection coefficient for duct open termination;  $t = 300\text{ }^{\circ}\text{C}$ , Experiments (blue circles), FEM - conical model (green diamonds), FEM - cylindrical model (pink stars)

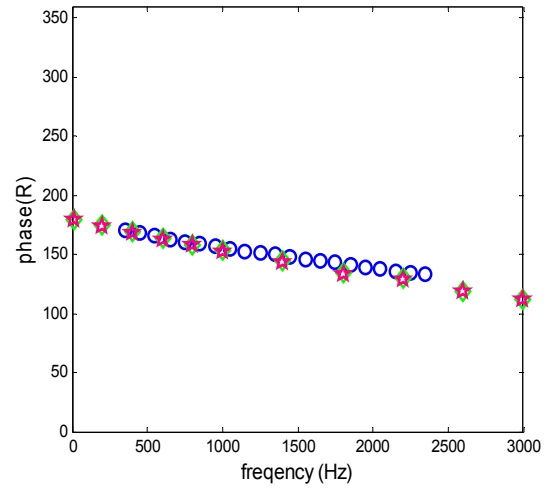


Figure 10. The phase of the reflection coefficient for duct open termination;  $t = 300\text{ }^{\circ}\text{C}$ , Experiments (blue circles), FEM - conical model (green diamonds), FEM - cylindrical model (pink stars)

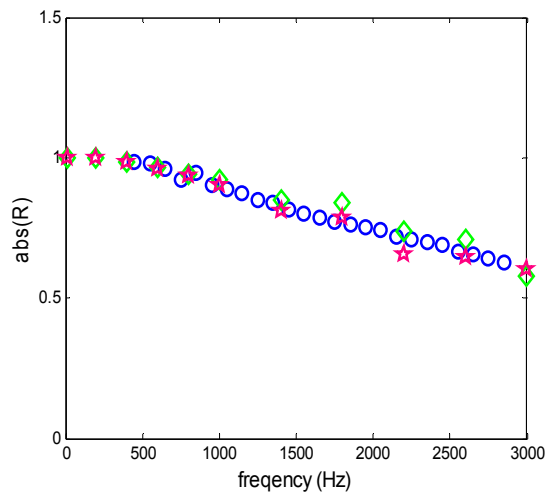


Figure 11. The magnitude of the reflection coefficient for duct open termination;  $t = 500\text{ }^{\circ}\text{C}$ , Experiments (blue circles), FEM - conical model (green diamonds), FEM - cylindrical model (pink stars)

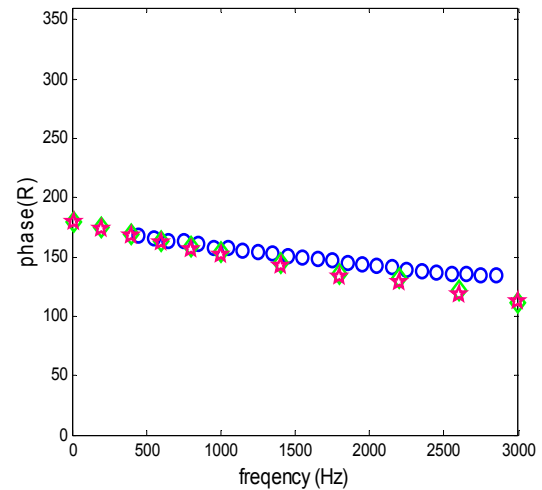


Figure 12. The phase of the reflection coefficient for duct open termination;  $t = 500\text{ }^{\circ}\text{C}$ , Experiments (blue circles), FEM - conical model (green diamonds), FEM - cylindrical model (pink stars)

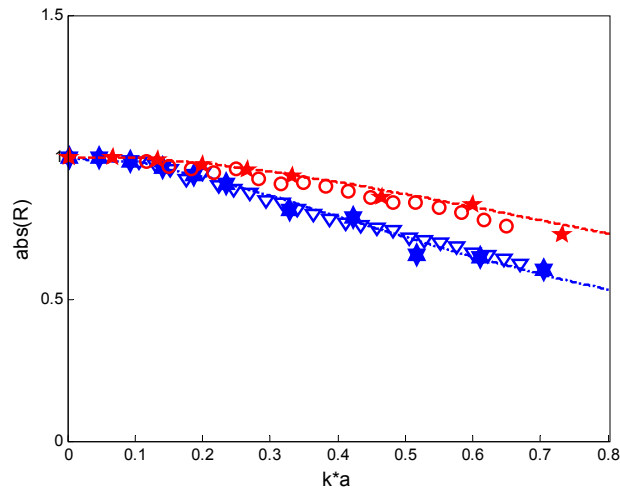


Figure 13. The magnitude of the reflection coefficient for open duct termination presented in Helmholtz number domain; Experiments,  $t = 100\text{ }^{\circ}\text{C}$  (red circles), FEM, cylindrical model,  $t = 100\text{ }^{\circ}\text{C}$  (red stars), Munt's theory,  $t = 100\text{ }^{\circ}\text{C}$  (red dashed line), Experiments,  $t = 500\text{ }^{\circ}\text{C}$  (blue triangles), FEM, cylindrical model,  $t = 500\text{ }^{\circ}\text{C}$  (blue hexagrams), Munt's theory,  $t = 500\text{ }^{\circ}\text{C}$  (blue dash-dotted line).

## 6. CONCLUSIONS

A numerical analysis has been performed for predicting the reflection coefficient of circular duct exhausting hot jet. A three dimensional model was created to represent the experimental conditions recently exerted by the authors to determine the acoustical passive properties of the open duct termination in hot conditions.

Despite of relatively simple linear FEM model with neglected flow effects the numerical results were in good agreement with the experimental ones. In a frequency domain the reflection coefficient magnitude is almost independent of the jet temperature, likewise the phase angle linked to the acoustical end correction of the duct. It was also demonstrated that at low Mach number and Helmholtz number cases the results agree well with the well-known Munt's model.

## REFERENCES

- [1] H. Rämmal, J. Lavrentjev, "Sound reflection at an open end of a circular duct exhausting hot gas", *Proceedings of the 35<sup>th</sup> International Congress on Sound and Vibration, Internoise 2006*, 3-6 December 2006, Honolulu, USA.
- [2] R. M. Munt, "Acoustic transmission properties of a jet pipe with subsonic jet flow: 1. The cold jet reflection coefficient", *Journal of Sound and Vibration*, **142**, 413-436 (1990).